IEEE Access
Multidisciplinary | Rapid Review | Open Access Journal

Received May 6, 2021, accepted June 8, 2021, date of publication June 30, 2021, date of current version July 14, 2021.

*Digital Object Identifier 10.1109/ACCESS.2021.3093720*

# Low-SAR Antenna Design and Implementation for Mobile Phone Applications

**BAO LU[1], BO PANG[2], WEI HU[2], (Member, IEEE), AND WEN JIANG[2], (Member, IEEE)**
[1]Guangdong OPPO Mobile Telecommunications Corporation Ltd., Dongguan 523000, China
[2]National Laboratory of Science and Technology on Antennas and Microwaves, Xidian University, Xi'an 710071, China

Corresponding author: Bo Pang (bpang@stu.xidian.edu.cn)

This work was supported by OPPO Mobile Telecommunications Corporation Ltd., China.

**ABSTRACT** This paper presents a novel approach for designing low-SAR (specific absorption rate) terminal antenna. First of all, the relationship between the magnetic field and the SAR value is deduced by using the electric field formula of SAR and Maxwell's equations. Then, by using the boundary conditions of the medium, the interaction mechanism between the radiated magnetic field of the antenna and the magnetic field inside human tissue is studied. Next, the relationship between the surface current and the radiated magnetic field of antenna is constructed. The approach of reducing the antenna radiated magnetic field is proposed by directly adjusting the antenna surface current, so that the SAR of human tissues is reduced. Finally, two low-SAR antennas are designed according to the proposed approach. The simulation and measurement results of the two low-SAR antennas show that the −6 dB bandwidth of both antennas is 2.4-2.49 GHz, which can meet the 2.4 G WLAN frequency band. At the same time, compared with the reference antenna, the peak values of 10 g average SAR of two antennas are reduced by more than 30%. In addition, the measured efficiencies of the two low-SAR antennas are higher than 40% in the operating frequency range. The validity of the proposed approach is proved by the simulation and measurement results of the antenna, which can be used to guide the SAR reduction design of mobile terminal antennas.

**INDEX TERMS** Inverted-F antenna, low SAR value, metal rim, mobile terminal applications.

## I. INTRODUCTION

After decades of vigorous development of mobile communication technology, various wireless terminal devices have been rapidly popularized, such as smart phones, smart watches, and tablet computers. These terminal devices have improved the quality and frequency of human information communication and greatly facilitated human daily life. When people use mobile phones for information exchange, electromagnetic waves are continuously sent and received between the mobile phone and the base station. Because human skin, muscle, fat and other tissues are all lossy media, human tissues can absorb and lose electromagnetic energy when exposed to electromagnetic waves. Once the absorbed electromagnetic energy exceeds a certain safety limit, human health will be seriously affected, such as impaired organ function, abnormal endocrine system, etc. Therefore, the electromagnetic radiation safety problem caused by wireless terminal equipment has attracted more and more attention from all walks of life.

In order to avoid excessive electromagnetic energy causing harm to human health, the specific absorption rate (SAR) has been introduced to characterize how electromagnetic radiation affects the human body. Many countries and international organizations have set their safety standards for SAR value. There are two most widely used safety standards for SAR value, one is known as the American standard [1], and the other is known as the European standard [2].

To solve the potential electromagnetic radiation problem when people use mobile terminal equipment, researchers in the industry have done a lot of work. The most direct method is to use wave-absorbing or shielding materials on the inner or outer surface of the terminal equipment shell to avoid emitting electromagnetic signals to the human body [3]–[5]. This method usually affects the radiation efficiency, gain and bandwidth of the antenna. Some scholars proposed to design auxiliary antennas [6]–[9]. Two identical antennas are designed in the terminal equipment, according to different

The associate editor coordinating the review of this manuscript and approving it for publication was Santi C. Pavone.

usage scenarios, one of two antennas is excited and the other antenna is grounded to shield the electromagnetic radiation of terminal equipment. Other scholars design the metamaterial structure to reduce the radiation of terminal antenna to human tissues, such as electromagnetic band gap (EBG) structures [10]–[12], High-impedance surfaces [13] and splitting resonators (SRRs) [14], [15]. However, whether designing auxiliary antennas or metamaterials, additional design space is required, which requires a larger antenna system size, and it is difficult to obtain practical applications for the full-screen mobile terminals. In addition, metamaterials are generally narrow-band resonant structures, which are also difficult to meet the bandwidth requirements of terminal antennas. Furthermore, some scholars have analyzed the mechanism of the electromagnetic wave absorbing from the perspective of the electric field [16], and they proposed to reduce electromagnetic radiation of mobile terminal equipment to users by reducing the tangential component of electric field. But under different usage scenarios, the above method is difficult to achieve. In this paper, we will explore the approach of SAR reduction design of mobile phone antenna from the perspective of the magnetic field. Meanwhile, the reliability of the method is verified by designing two low SAR terminal antennas, which can be used to guide the SAR reduction design of mobile terminal antennas.

## II. THEORY FOR ANTENNA REDUCTION SAR DESIGN

### A. THE RELATION BETWEEN MAGNETIC FIELD AND SAR

SAR can be interpreted as the electromagnetic energy consumed by unit organization in a unit of time The local SAR is related to the internal electric field of tissues, so the internal electric field of tissues can be used to calculate the local SAR. The electric field calculation formula of the local SAR is:

$$SAR = \frac{\sigma |\mathbf{E}_{in}|^2}{2\rho_m} \tag{1}$$

where $\mathbf{E}_{in}$ represents the local electric field induced in human tissue under electromagnetic radiation. $\sigma$ represents the local electrical conductivity of human tissues. $\rho_m$ refers to the local mass density of human tissues.

The electromagnetic field radiated by the antenna into free space is a time-varying electromagnetic field. For time-varying electromagnetic fields, the magnetic field and electric field no longer maintain an independent relationship. The magnetic field and the electric field excite and transform each other to form a unified time-varying electromagnetic field, so the electric and magnetic fields inside biological tissues are constantly exciting and transforming each other. According to Maxwell's equations:

$$\nabla \times \mathbf{H}_{in} = j\omega\varepsilon\mathbf{E}_{in} \tag{2}$$

Incorporating the (2) into (1), the magnetic field calculation formula for calculating the SAR value is as follows:

$$SAR = \frac{\sigma}{2\rho_m}\frac{1}{\omega^2\varepsilon^2}|\nabla \times \mathbf{H}_{in}|^2 \tag{3}$$

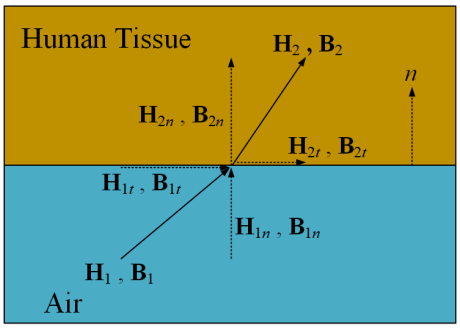


**FIGURE 1.** Boundary conditions.

where $\mathbf{H}_{in}$ is the induced magnetic field inside human tissues. $\varepsilon$ is the local dielectric constant of human tissues.

Therefore, the SAR value can be calculated using the electric field in the tissues or the magnetic field in the tissues, and the two calculation methods give the same result. So the induced electric field or the induced magnetic field in tissues will decide the SAR value. Here this paper will explore the relationship between the radiated magnetic field of terminal antenna and the induced magnetic field inside human tissues.

As shown in Figure 1, $n$ is the unit vector perpendicular to the interface between air and human tissue. $\mathbf{H}_1$ is the radiated magnetic field of terminal antenna. $\mathbf{H}_2$ refer to the induced magnetic field in human tissues. $\mathbf{B}_1$ is the magnetic flux of antenna in the air. $\mathbf{B}_2$ is induced magnetic flux inside human tissues. Based on the boundary conditions of the medium:

$$\begin{aligned} \mu_1 H_{1n} &= \mu_2 H_{2n} \\ B_{1n} &= B_{2n} \\ H_{1t} &= H_{2t} \\ B_{1t}/\mu_1 &= B_{2t}/\mu_2 \end{aligned} \tag{4}$$

where $H_{1n}$ is the normal components of the magnetic field on air side of interface between air and human tissue. $B_{1n}$ is the normal components of the corresponding magnetic flux. $B_{1t}$and $H_{1t}$ are the magnetic flux and the tangential components of magnetic field on air side of the boundary. $B_{2n}$ and $H_{2n}$ are the magnetic flux and the normal components of magnetic field and on human tissues side of the boundary. $B_{2t}$ and $H_{2t}$ are the magnetic flux and the tangential components of the magnetic field on human tissues side of the boundary. $\mu_1$ and $\mu_2$ refer to the magnetic permeability of air and human tissues, respectively.

According to relevant research reports [17], the magnetic materials are weakly magnetic in the human body and most other animals, so the magnetic permeability of the human body and most other animals is similar to the magnetic permeability of air, as follows:

$$\mu_1 = \mu_2 \tag{5}$$

Putting the (5) into (4), the following formula can be obtained:

$$H_{1n} = H_{2n}$$

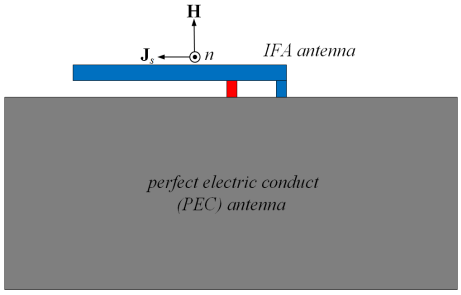


**FIGURE 2.** The Inverted-F antenna (IFA) antenna.

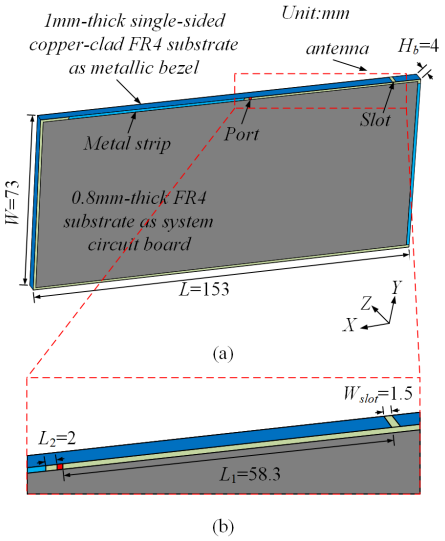


**FIGURE 3.** The structure and dimension of the reference antenna: (a) Perspective view, (b) Partial view (antenna).

$$\begin{aligned} B_{1n} &= B_{2n} \\ H_{1t} &= H_{2t} \\ B_{1t} &= B_{2t} \end{aligned} \tag{6}$$

Further finishing (6), the following formula can be obtained:

$$\begin{aligned} \mathbf{H}_1 &= \mathbf{H}_2 \\ \mathbf{B}_1 &= \mathbf{B}_2 \end{aligned} \tag{7}$$

It can be concluded that the tangential and normal components of the magnetic flux and magnetic field are continuous before and after entering the human tissues, and the magnetic field and magnetic flux will not change basically. Therefore, the SAR value of the antenna will be determined by the radiated magnetic field of the mobile terminal antenna. If the radiated magnetic field of the mobile terminal antenna is weakened, the SAR value of the antenna can be decreased. In the following, we will explore the direct factors that affect the radiated magnetic field of antenna.

### B. THE RELATION BETWEEN MAGNETIC FIELD AND CURRENT

Here we take the Inverted-F antenna (IFA) antenna as an example to explore the main factors affecting the magnetic field in the near field of the mobile terminal antenna. IFA antenna is composed of the ideal conductor. According to the basic theory of the electromagnetic field, there is no electromagnetic field inside the ideal conductor, and the electromagnetic field is only distributed outside the ideal conductor. As shown in Figure 2, $n$ represents the outer normal vector of the ideal conductor, $\mathbf{H}$ represents the surface magnetic field of the ideal conductor, $\mathbf{J_s}$ represents the surface current density of ideal conductor. According to the boundary conditions of ideal conductor surface:

$$\mathrm{n} \times \mathbf{H} = \mathbf{J}_\mathrm{s} \tag{8}$$

It can be obtained from the (8) that the surface current density of an ideal conductor determines the intensity of the radiant magnetic field generated by it.

Therefore, the surface current distribution of the antenna is the main factor that determines the amplitude of the antenna radiated magnetic field. The larger the surface current on the antenna, the greater the magnetic field radiated by the antenna. The stronger the magnetic field radiated by the antenna, the larger the induced magnetic field in the biological tissue, and the greater the SAR value of the antenna. So as long as the surface current density of the antenna radiator is reduced, the antenna will have a lower SAR value.

## III. LOW-SAR ANTENNA DESIGN AND IMPLEMENTA-TION

### A. REFERENCE ANTENNA

In order to verify the proposed design method can achieve terminal antenna SAR reduction, a metal-rimmed terminal antenna is proposed as a reference antenna. The structure and dimension of the reference antenna is given in Figure 3. As shown in Figure 3 (a), the system circuit board adopts the 0.8mm thick FR4 dielectric board commonly used in the industry. Four FR4 substrates with a thickness of 1 mm are adopted to imitate the realistic metallic bezels. The system circuit board is perpendicular to the four metallic bezels. The dimension of the system circuit board is 151 $\times$ 71 mm$^2$ and four metallic bezels have a uniform height of 4mm. The antenna is designed by adding a feed port and a grounded metal strip on the long side of the metal frame and the dimension of the metal frame antenna is given in Figure 3 (b).

In the following of this paper, we will use two methods to adjust the current of the reference antenna to weaken the magnetic field radiated by the terminal antenna, and finally achieve the SAR reduction design of the terminal antenna. In the following, the reference antenna will be referred to as Antenna 1 for the convenience of writing.

### B. LOW-SAR DESIGN I

According to the approach in section II, the SAR value is decided by the radiated magnetic field of the terminal antenna. However, the surface current density on the antenna directly affects the radiated magnetic field of the antenna. In this paper, the parasitic branch is added to the strong

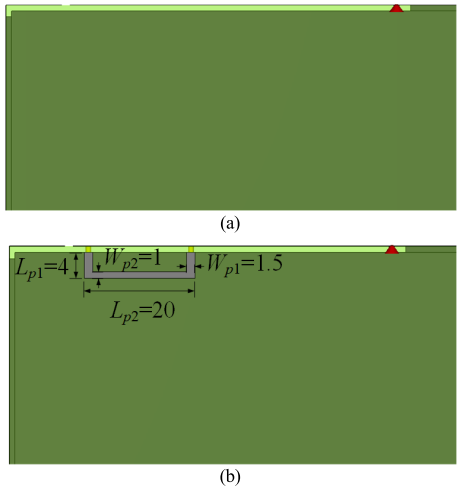


**FIGURE 4.** Geometry and dimension of Antenna 1 and Antenna 2.

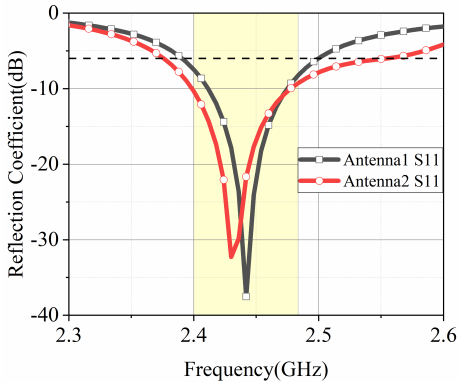


**FIGURE 5.** Simulated S11 of Antenna 1 and Antenna 2.

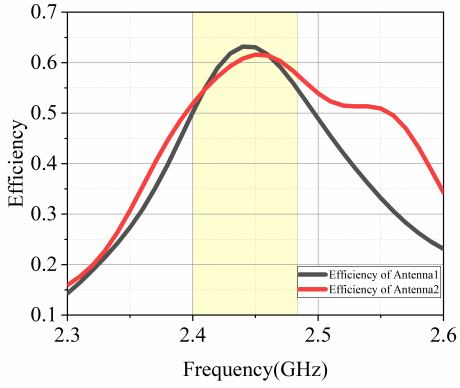


**FIGURE 6.** Simulated efficiency of Antenna 1 and Antenna 2.

current area, to make the current propagate through multiple paths, which achieve uniform distribution of the antenna current. To illustrate the effect of adding parasitic branch, the characteristics of the Antenna 1 and the Antenna 2 in Figure 4 are compared. The simulated S11 curves of Antenna 1 and Antenna 2 are given in Figure 5. It can be seen from Figure 5, the −6 dB operating band of Antenna2 is slightly narrower than that of Antenna 1 and both antennas can meet the required frequency band of 2.4G WLAN (2.4-2.49 GHz).

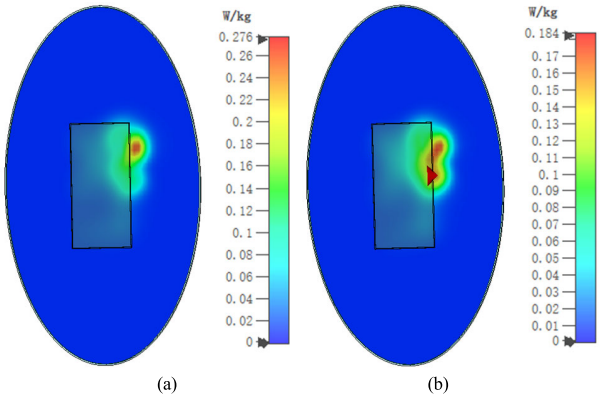


**FIGURE 7.** 10 g average SAR of both antennas at 2.45 GHz (accepted power is 14 dBm): (a) Antenna 1, (b) Antenna 2.

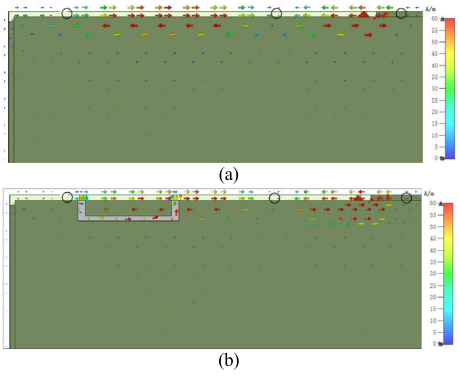


**FIGURE 8.** The surface current distributions of Antenna 1 and Antenna 2 at 2.45GHz.

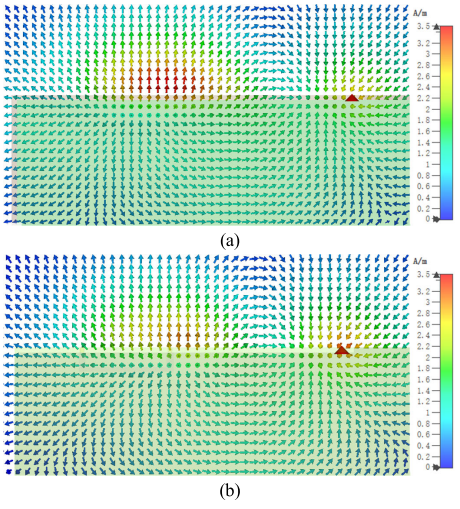


**FIGURE 9.** The magnetic field distributions on the reference plane of Antenna 1 and Antenna 2 at 2.45 GHz.

The reason is that the loading parasitic branch affects the impedance matching of Antenna 2. The simulated efficiency curves of Antenna 1 and Antenna 2 are given in Figure 6. Their efficiencies are basically the same and above 50% in 2.4 G WLAN band.

The SAR distributions of both antennas at 2.45 GHz are shown in Figure 7. A simplified human tissue model is

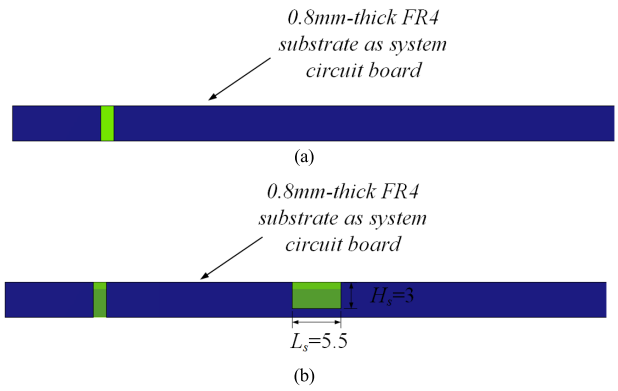


**FIGURE 10.** The structure of (a) Antenna 1, (b) Antenna 3.

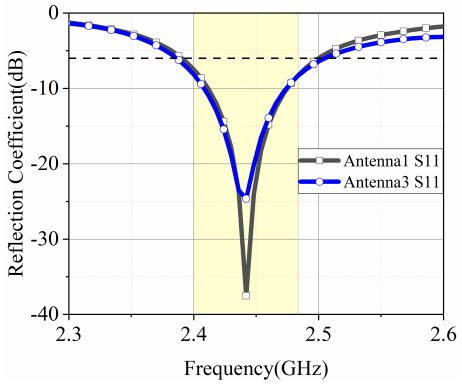


**FIGURE 11.** Simulated S11 of Antenna 1 and Antenna 3.

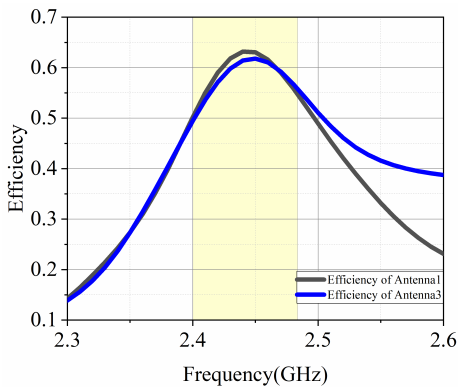


**FIGURE 12.** Simulated efficiency of Antenna 1 and Antenna 3.

established based on the IEEE Std 1528-2003 [18]. The two antennas were placed 5mm above the human tissue model. The accepted power of the two antennas is 14 dBm, the peak values of 10 g average SAR of Antenna 1 at 2.45 GHz is 0.276 W/kg while the peak SAR value of Antenna 2 is 0.184 W/kg Therefore, compared with the Antenna 1, the 10g average SAR peak value of the Antenna 2 is reduced by 33.3%, achieving a significant SAR reduction effect.

Figure 8 shows the current distribution of the two antennas at 2.45GHz. It can be seen that the current distributions of both antennas are the same basically, and which of them have three zero points. It shows that both antennas work in

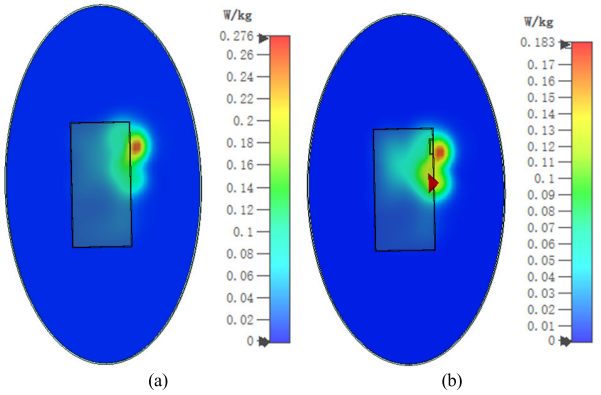


**FIGURE 13.** 10 g average SAR of both antennas at 2.45 GHz (accepted power is 14 dBm): (a) Antenna 1, (b) Antenna 3.

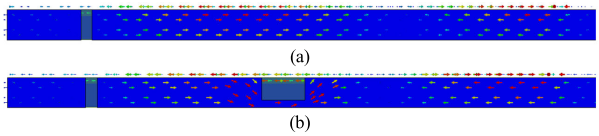


**FIGURE 14.** The surface current distributions of Antenna 1 and Antenna 3 at 2.45GHz.

the3/4λ mode at the resonance frequency. The Antenna 2 is constructed by introducing parasitic branch based on Antenna 1, and the Antenna 2 has strong current distribution on and the parasitic branch and the metal frame, as shown in Figure 8 (b).

In order to explain the mechanism of SAR reduction, the magnetic field distribution of the two antennas at 2.45GHz is also analyzed. This paper selects the plane directly below the antenna and 5mm away from the antenna as the reference plane. The magnetic field distributions of both antennas on the reference plane are given as shown in Figure 9. It can be found that the magnetic field of Antenna 2 (with the branch) at the position where the parasitic branch is added is significantly weaker than that of Antenna 1 (without the branch). Therefore, according to the SAR reduction design method proposed in this article, the current density of the mobile terminal antenna will be weakened by loading the parasitic branch, result in a lower induced magnetic field and a lower SAR value.

### C. LOW-SAR DESIGN II

In this part, another method will be used to control the surface current of antenna. The rectangular slot is loaded in the strong current area of the antenna, so that the surface current of the antenna is far away from the human body tissues, and the radiated magnetic field of the antenna to the human body will be weakened. As shown in Figure 10, there are the geometry and dimension of the Antenna 1 and Antenna 3. The dimension of the rectangular slot is shown in Figure 10 (b). To illustrate the effect of adding rectangular slot, properties of the Antenna 1 without the rectangular slot and the Antenna 3 with the rectangular slot in Figure 10 are compared.

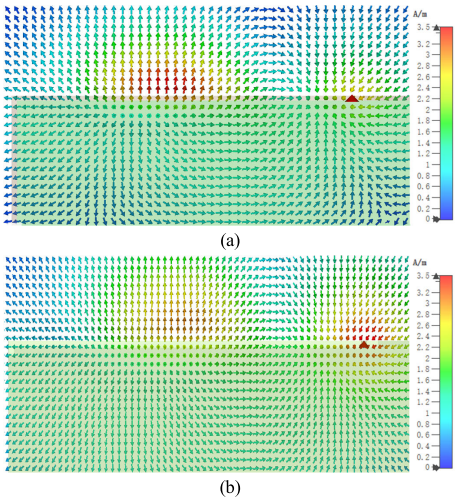

**FIGURE 15.** The magnetic field distributions on the reference plane of Antenna 1 and Antenna 3 at 2.45 GHz.

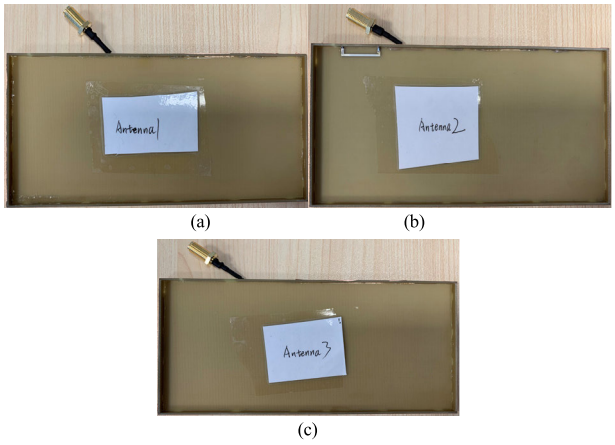


**FIGURE 16.** The photographs of the fabricated Antenna 1, Antenna 2 and Antenna 3.

The simulated S11 curves of both antennas are given in Figure 11. It can be seen from Figure 11, the −6 dB operating band of Antenna 3 is slightly narrower than that of Antenna 1 and both antennas can meet the required frequency band of 2.4 G WLAN (2.4-2.49 GHz). The reason is that the rectangular slot affects the impedance performance of the Antenna 3. The simulated efficiency curves of both antennas are given in Figure 12. Their efficiencies are basically the same, and the efficiencies in the working frequency band are more than 50% in 2.4 G WLAN band.

The SAR distributions of both antennas at 2.45 GHz are shown in Figure 13. Also, the two antennas were placed 5mm above the human tissue model. The accepted power of the two antennas is 14 dBm, the peak values of 10 g average SAR of Antenna 1 at 2.45 GHz is 0.276 W/kg, while the SAR peak value of Antenna 3 is 0.183 W/kg. Therefore, compared with the Antenna 1, the 10g average SAR peak value of the Antenna 3 is reduced by 33.7%, achieving a significant SAR reduction effect.

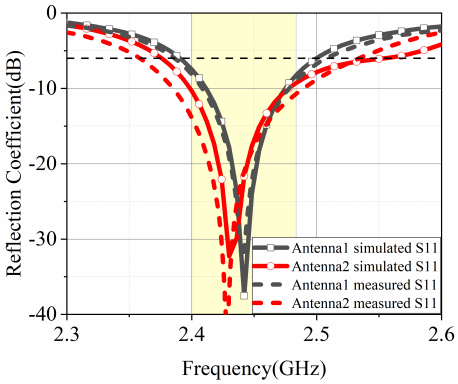


**FIGURE 17.** Simulated and measured S11 of Antenna 1 (without the branch) and Antenna 2 (with the branch).

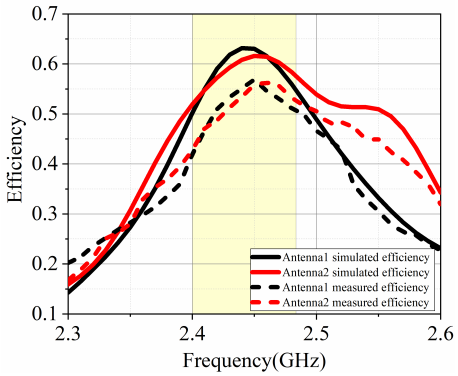


**FIGURE 18.** Simulated and measured efficiency of Antenna 1 and Antenna 2.

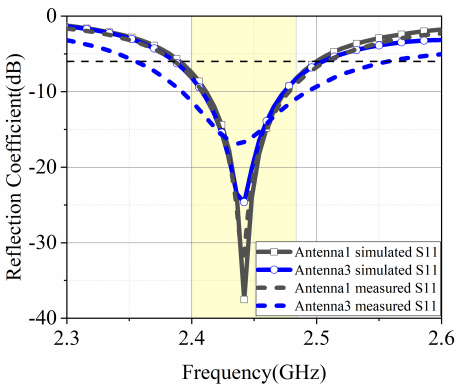


**FIGURE 19.** Simulated and measured S11 of Antenna 1 and Antenna 3.

**TABLE 1.** The simulation and measurement SAR peak values of the proposed antennas.

| | Antenna1 | Antenna2 | Antenna3 |
|---|---|---|---|
| Body(simulated) | 0.276 | 0.184 | 0.183 |
| Body(Measured) | 0.275 | 0.178 | 0.152 |

The surface current distributions of both antennas (Antenna 1 and Antenna 3) at 2.45GHz are shown in Figure 14, and the surface current distributions on the meta frame of the two antennas are basically the same. Compared with the Antenna 1, the current distribution on the Antenna 3 is far away from the system circuit board by loading the

**TABLE 2.** Comparison of the proposed work with other SAR reduction work.

| Ref. | Reduction SAR method | Frequency | Simulated Efficiency | Additional space | SAR Reduction |
|---|---|---|---|---|---|
| [3] | Wave-absorbing Material | 900MHz | - | Yes | 10-25% |
| [4] | Wave-absorbing Material | 1.83GHz | - | Yes | 15-65% |
| [5] | Wave-absorbing Material | 1800MHz | 38% | Yes | 88% |
| [6] | Reflector | 900MHz | - | Yes | 30-44% |
| [7] | Reflector | 900MHz | 71% | Yes | 66% |
| [11] | EBG | 3.5GHz | 91% | Yes | 84% |
| [12] | EBG | 1.88GHz | - | Yes | 31% |
| [14] | SRRs | 900MHz and 1800MHz | - | Yes | 27.57%-37.62% |
| [15] | SRRs | 900MHz | - | Yes | 42.12% |
| This Work | Adjusting the Distribution of Magnetic Field | 2.45GHz | 61.6% and 61.8% | No | 33.3% and 33.7% |

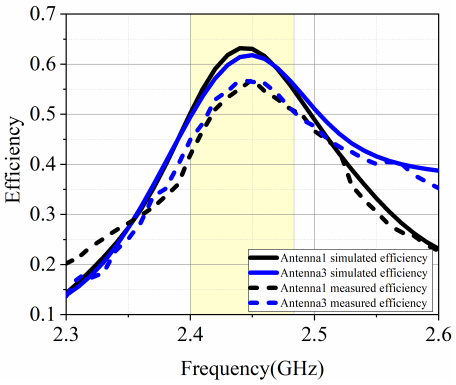


**FIGURE 20.** Simulated and measured efficiency of Antenna 1 and Antenna 3.

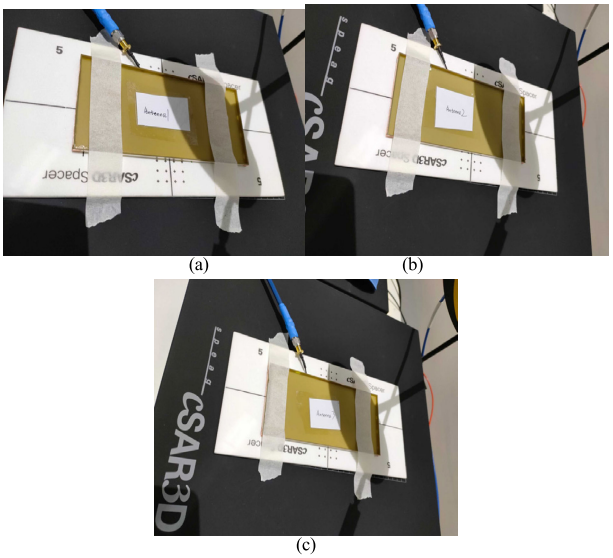


**FIGURE 21.** The photograph of SAR measurement setup.

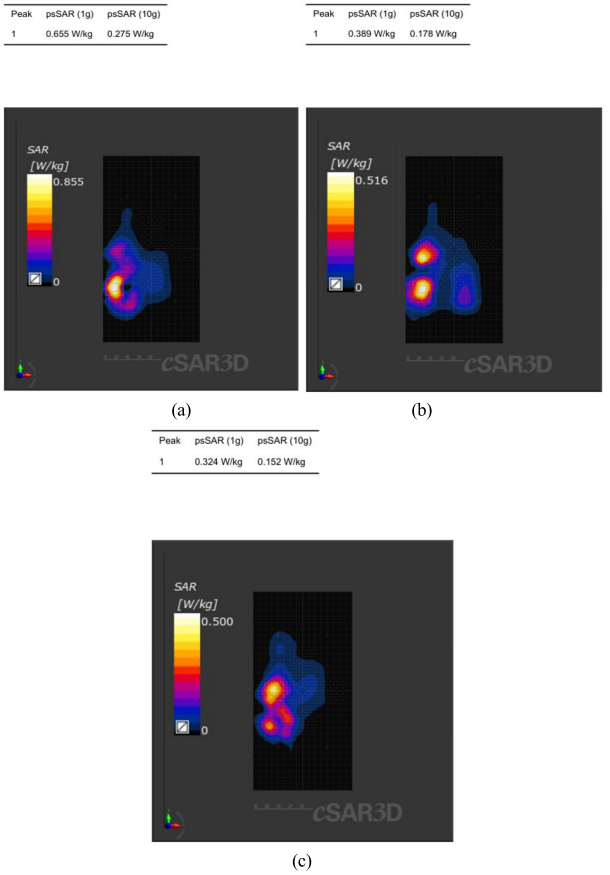


**FIGURE 22.** Measured 10 g average SAR of the proposed antennas (input power is 14 dBm): (a) Antenna 1, (b) Antenna 2, (c) Antenna 3.

rectangular slot structure as shown in Figure 14(b). The human body is located under the system circuit board, so the current distribution on the Antenna 3 can be far away from the human body through the loading rectangular slot.

The magnetic field distributions of the two antennas at 2.45 GHz are also analyzed. Also, we select the plane directly below the antenna and 5mm away from the antenna as the reference plane. The magnetic field distributions of the both antennas on the reference plane are given as shown in Figure 15. It can be found that the magnetic field of Antenna 3 at the position where the rectangular slot is added is significantly weaker than that of Antenna 1 (without the rectangular slot). Therefore, according to the SAR reduction design method proposed in this paper, the current distribution of the antenna will far away from the human body by loading the rectangular slot, result in a lower induced magnetic field and a lower SAR value.

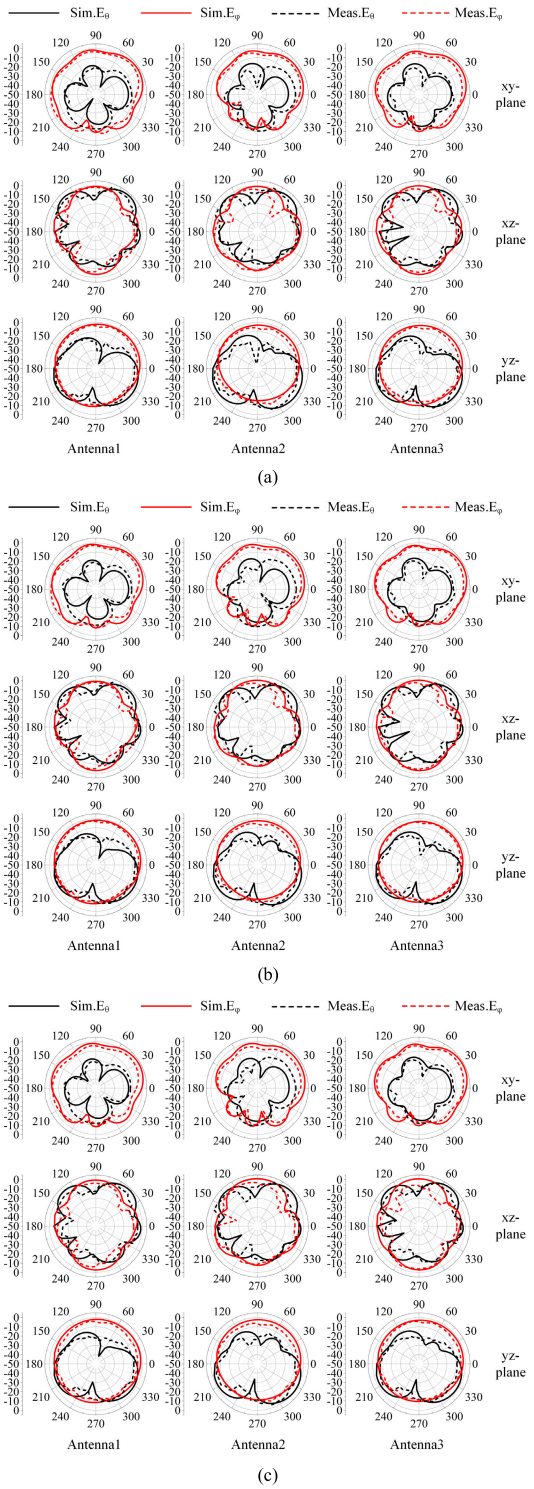


**FIGURE 23.** Measured radiation patterns at three frequency points: (a) 2.4GHz, (b) 2.45GHz, (c) 2.48GHz.

### D. PERFORMANCE OF THE PROPOSED ANTENNAS

Figure 16 shows photographs of the fabricated antennas. The simulation and measurement S11 curves of Antenna 1 (without the branch) and Antenna 2 (with the branch) are given in Figure 17. The measured S11 curves agree well with the simulated results. From the measured S11 results, the S11 ($<-6$ dB) bandwidth of the Antenna 1 is from 2.39 GHz to 2.50 GHz, and which of the fabricated Antenna 2 is from 2.36 GHz to 2.53 GHz. Both of antennas can meet the desired 2.4 G WLAN band (2.4-2.49 GHz). According to Figure 18, the efficiencies in simulation and measurement of both antennas in the 2.4 G WLAN are above 40%. Due to manufacturing error and dielectric loss, the antenna simulation results and test results are different. Figure 19 shows the simulation and measurement S11 curves of Antenna 1 (without rectangular slot) and Antenna 3 (with rectangular slot). The measured reflection coefficient agrees with the simulated result basically. The $-6$ dB bandwidth of fabricated Antenna 3 is 2.36-2.55 GHz, which can meet the desired 2.4 G WLAN band (from 2.4 GHz to 2.49 GHz). The simulation and measurement total efficiencies of the Antenna 1 and Antenna 3 are given as shown in Figure 20, which are above 40% in the operating frequency band. Reasons for the big difference about measurement and the simulation of the Antenna 3 is also due to the manufacturer errors and dielectric loss.

The photograph of SAR measurement setup is shown in Figure 21. Figure 22 shows measured 10 g average SAR of the fabricated antennas. The test power of the antennas is 14 dBm. Comparing Figure 7, Figure 13 and Figure 22, It can be seen that the measured SAR distributions of the antennas agrees well with the simulated results. The simulation and measurement 10 g average SAR peak values of the antennas at 2.45 GHz are recorded as shown in Table 1. It can be found that the SAR peak values of both proposed low-SAR antennas are decreased by more than 30%, compared with the reference antenna.

As shown in Figure 23, the measured and simulated radiation patterns of proposed antennas at three frequencies in the three principal planes are given. The measured radiation patterns agree reasonably well with the simulated results. As observed from the figure, adding the parasitic branch and the rectangular slot do not change the radiation pattern of the original antenna.

It is a comparison between the previous low SAR design work and the proposed low SAR design work, as shown in Table 2. In [5], absorbing materials are used to achieve the low SAR design of the antenna, but adding wave-absorbing material will deteriorate the efficiency of the antenna. The rest of the reported work has designed various SAR reduction structures to reduce the SAR value of the antennas, which requires additional design space. The proposed work achieves a low SAR design without affecting the antenna efficiency, which does not require an additional SAR reduction structure.

## IV. CONCLUSION

The SAR reduction design method of mobile terminal antennas is studied in the paper. According to the mutual excitation and mutual transformation of the electric field and the magnetic field in the time-varying electromagnetic field, the magnetic field calculation formula of the antenna SAR value is derived. Through using the boundary conditions of

the medium, the relationship between the radiated magnetic field of the terminal antenna and the magnetic field in human tissue is analyzed. It can be concluded that the SAR distributions of the mobile terminal antenna is closely connected with the radiated magnetic field strength and distribution of the antenna. We further find that the current distribution on the surface of the antenna is directly related to the magnetic field distributions of the antenna. Furthermore, this paper proposes two methods to adjust the surface current distribution of the antenna to decrease the radiated magnetic field of the antenna and achieve a lower SAR value. Finally, two low-SAR antennas for mobile terminals are designed according to these two methods. The results of Simulation and measurement show that the SAR peak values of both low-SAR antennas are weaken by over 30% compared with the original antenna. The theories and methods presented in this paper can be used to guide the SAR reduction design for terminal antennas.

## REFERENCES

[1] *IEEE Standard for Safety Levels With Respect to Human Exposure to Radio Frequency Electromagnetic Fields, 3 kHz to 300 GHz*, IEEE Standard C95.1-2005, Apr. 2006.
[2] International Commission on Non-Ionizing Radiation Protection, "Health issues related to the use of hand-held radiotelephones and base transmitters," *Health Phys.*, vol. 70, no. 4, pp. 587–593, Apr. 1996.
[3] J. Wang, O. Fujiwara, and T. Takagi, "Effects of ferrite sheet attachment to portable telephone in reducing electromagnetic absorption in human head," presented at the IEEE Int. Symp. Electromagn. Compatability. Symp. Rec., Aug. 1999. [Online]. Available: https://ieeexplore.ieee.org/document/810126/references#references
[4] M. Jung and B. Lee, "SAR reduction for mobile phones based on analysis of EM absorbing material characteristics," presented at the Antennas Propag. Soc. Int. Symp., 2003. [Online]. Available: https://ieeexplore.ieee.org/document/1219407
[5] M. I. Kitra, C. J. Panagamuwa, P. McEvoy, J. C. Vardaxoglou, and J. R. James, "Low SAR ferrite handset antenna design," *IEEE Trans. Antennas Propag.*, vol. 55, no. 4, pp. 1155–1164, Apr. 2007.
[6] J. Ilvonen, R. Valkonen, O. Kiveks, P. Li, and P. Vainikainen, "Antenna shielding method reducing interaction between user and mobile terminal antenna," *Electron. Lett.*, vol. 47, no. 16, pp. 896–897, 2011.
[7] R. Y.-S. Tay, Q. Balzano, and N. Kuster, "Dipole configurations with strongly improved radiation efficiency for hand-held transceivers," *IEEE Trans. Antennas Propag.*, vol. 46, no. 6, pp. 798–806, Jun. 1998.
[8] A. Hirata, T. Adachi, and T. Shiozawa, "Folded-loop antenna with a reflector for mobile handsets at 2.0 GHz," *Microw. Opt. Technol. Lett.*, vol. 40, no. 4, pp. 272–275, Feb. 2004.
[9] M. Bank and B. Levin, "The development of a cellular phone antenna with small irradiation of human-organism tissues," *IEEE Antennas Propag. Mag.*, vol. 49, no. 4, pp. 65–73, Aug. 2007.
[10] S. I. Kwak, D. U. Sim, J. H. Kwon, and H. D. Choi, "Experimental tests of SAR reduction on mobile phone using EBG structures," *Electron. Lett.*, vol. 44, no. 9, pp. 568–569, Apr. 2008.
[11] R. Ikeuchi and A. Hirata, "Dipole antenna above EBG substrate for local SAR reduction," *IEEE Antennas Wireless Propag. Lett.*, vol. 10, pp. 904–906, 2011.
[12] S. I. Kwak, D.-U. Sim, and J. H. Kwon, "Design of optimized multilayer PIFA with the EBG structure for SAR reduction in mobile applications," *IEEE Trans. Electromagn. Compat.*, vol. 53, no. 2, pp. 325–331, May 2011.
[13] R. F. J. Broas, D. F. Sievenpiper, and E. Yablonovitch, "A high-impedance ground plane applied to a cellphone handset geometry," *IEEE Trans. Microw. Theory Techn.*, vol. 49, no. 7, pp. 1262–1265, Jul. 2001.
[14] J.-N. Hwang and F.-C. Chen, "Reduction of the peak SAR in the human head with metamaterials," *IEEE Trans. Antennas Propag.*, vol. 54, no. 12, pp. 3763–3770, Dec. 2006.
[15] M. Tariqul, N. Misran, T. Sue, and M. Rashed, "Reduction of specific absorption rate (SAR) in the human head with materials and metamaterial," in *Proc. Int. Conf. Electr. Eng. Informat.*, Selangor, Malaysia, Aug. 2009, pp. 707–710.
[16] H. H. Zhang, G. G. Yu, Y. Liu, Y. X. Fang, G. Shi, and S. Wang, "Design of low-SAR mobile phone antenna: Theory and applications," *IEEE Trans. Antennas Propag.*, vol. 69, no. 2, pp. 698–707, Feb. 2021.
[17] F. Mei, "Biological magnetic phenomena and magnetic effects and their applications," in *Modern Physics Knowledge*. Beijing, China: Science Press, 2004.
[18] A. M. M. Salem, *IEEE Recommended Practice for Determining the Peak Spatial-Average Specific Absorption Rate (SAR) in the Human Head From Wireless Communications Devices: Measurement Techniques—Amendment 1: CAD File for Human Head Model (SAM Phantom)*, IEEE Standard 1528a-2005, Feb. 2006. [Online]. Available: https://ieeexplore.ieee.org/document/1603350

**BAO LU** received the Ph.D. degree in electromagnetic fields and microwave technology from Xidian University, Xi'an, China, in 2011. From 2011 to 2018, he was an Antenna Specialist at Huawei Technologies. In 2018, he joined OPPO Communication Technologies, where he is currently a Mobile Antenna Expert. His current research interests include small antennas and mm-wave phased array antennas for 5G mobile terminals. He is the Antenna Division Committee Member of the Chinese Institute of Electronic.

**BO PANG** received the B.S. degree in electronic science and technology from the Guilin University of Electronic Technology, Guilin, China, in 2016. He is currently pursuing the Ph.D. degree in electromagnetic wave and microwave technology with Xidian University, Xi'an, China.

**WEI HU** (Member, IEEE) received the Ph.D. degree in electromagnetic fields and microwave technology from Xidian University, Xi'an, China, in 2013. From 2013 to 2017, he was a Lecturer with the National Key Laboratory of Antennas and Microwave Technology, Collaborative Innovation Center of Information Sensing and Understanding, Xidian University, where he is currently an Associate Professor. From 2018 to 2019, he visited the University of Kent, U.K., as an Academic Visitor. He has authored and coauthored more than 70 internationally refereed journal articles. He has been serving as a reviewer for a number of technical journals and international conferences. His current research interests include multiband and wideband antennas, circularly polarized antennas, MIMO antenna arrays, and wideband wide-scanning phased arrays.

**WEN JIANG** (Member, IEEE) was born in Shandong, China, in November 1985. He received the B.S. and Ph.D. degrees from Xidian University, Xi'an, China, in 2008 and 2012, respectively. He is currently the Vice Director with the National Key Laboratory of Science and Technology on Antennas and Microwaves, Xidian University. He is also a Full Professor with Xidian University. His current research interests include electromagnetic scattering theory and technology, antenna theory and engineering, and electromagnetic measurement theory and technology.